Research Article | Vol. 28, No. 12 / 8 June 2020 / Optics Express 17570
Optics EXPRESS

All-fiber short-wavelength tunable mode-locked fiber laser using normal dispersion thulium-doped fiber

SHAOXIANG CHEN, YUHAO CHEN, KUN LIU, RAGHURAMAN SIDHARTHAN, HUIZI LI, CHEN JIAN CHANG, QI JIE WANG, DINGYUAN TANG, AND SEONGWOO YOO*

School of Electrical and Electronic Engineering, The Photonics Institute, Nanyang Technological University, 639798, Singapore
seon.yoo@ntu.edu.sg

Abstract: We report an all-fiber high pulse energy ultrafast laser and amplifier operating at the short wavelength side of the thulium (Tm) emission band. An in-house W-type normal dispersion Tm-doped fiber (NDTDF) exhibits a bending-induced distributed short-pass filtering effect that efficiently suppresses the otherwise dominant long wavelength emission. By changing the bending diameter of the fiber, we demonstrated a tunable mode-locked Tm-doped fiber laser with a very wide tunable range of 152 nm spanning from 1740 nm to 1892 nm. Pulses at a central wavelength of 1755 nm were able to be amplified in an all-fiber configuration using the W-type NDTDF, without the use of any artificial short-pass filter or pulse stretcher. The all-fiber amplifier delivers 2.76 ps pulses with an energy of ~32.7 nJ without pulse break-up, due to the normal dispersion nature of the gain fiber, which marks so far, the highest energy amongst fiber lasers in the 1700 nm-1800 nm region.

© 2020 Optical Society of America under the terms of the OSA Open Access Publishing Agreement

1. Introduction

Compared with the conventional excitation wavelengths of ~800 nm and 1300 nm, the third near-infrared (NIR-III) optical window (1600-1850 nm) offers an enhanced attenuation length for bio-imaging applications [1]. Recently, development of laser sources at near 1700 nm in the NIR-III window has been intensively investigated to enable deeper penetration depth for high-resolution optical imaging applications such as three-photon microscopy (3PM) and optical coherent tomography [2–4]. The 3PM requires high energy ultrafast pulses to facilitate the three-photon absorption in the NIR-III region. In addition, wavelength tunability is being in demand to increase the number of accessible fluorophores. Moreover, several strong absorption lines relating to the O-H, C-O and C-H bond resonances are present in the 1700- 1800 nm [5,6], rendering opportunities of photoacoustic imaging and plastic processing applications. In the past, several efforts were made to achieve high pulse energy ultrafast fiber lasers in the NIR-III region. Wang et al. demonstrated soliton self-frequency shift in a large mode area fiber to reach a pulse energy of < 20 nJ in the 1700-1800 nm region, but at the expense of indispensable bulk components in conjunction with a high-energy femtosecond pump source [7]. Alternatively, a quest for new gain medium in the 1700 nm region was explored in a high-GeO_2 silica-based bismuth-doped fiber (BDF). T. Noronen et al. reported an ultrafast BDF laser in the 1700 nm region, but with a low energy of sub nJ from an oscillator [8]. Power scaling through the BDF appears impeded by the little understood origin of the Bi emission in the NIR-III region, in other words low gain and inevitably long fiber length [9]. On the other hand, a silica-based thulium-doped fiber (TDF), with its broad emission spanning from 1600 to 2100 nm in the $^3F_4$-$^3H_6$ transition, is a promising gain medium to achieve ultrafast pulse lasers in the NIR-III region. Nevertheless, realization of a TDF laser below 1800 nm has been challenging

#395167 https://doi.org/10.1364/OE.395167
Journal © 2020 Received 15 Apr 2020; revised 18 May 2020; accepted 18 May 2020; published 27 May 2020

Optics EXPRESS

due to the strong reabsorption from the quasi-three-level nature and dispersion induced pulse energy limit. To achieve the short wavelength operation using silica-based TDF, amplified spontaneous emission (ASE) at long wavelengths (above 1800 nm) has to be suppressed by incorporating short-pass filters of bulk components, co-doping of an absorbing ion such as holmium (Ho) [10], or fiberized short-pass filters, such as coiled dispersion compensating fiber (DCF) [11] or a photonic crystal fiber [12]. Insertion of the extra filters increases complexity of the cavity and also induce additional insertion loss at the desired 1700 nm region. Furthermore, energy scaling in the 1700-1800 nm is also limited by the anomalous dispersion in a silica fiber. The pulse energy scalability can be improved when overall cavity dispersion is managed by employing a dispersion compensating passive fiber to generate dispersion-managed soliton or dissipative soliton. Nonetheless, the pulse energy limit still stands owing to the significant anomalous-dispersion and/or low gain in an active fiber, or TDF, in the NIR-III region [13]. Consequently, the state-of-the-art demonstrations were only able to produce ~14.9 nJ pulse energy from a fiber laser system [14]. An efficient gain fiber offering normal dispersion in this region would be more desired for energy scaling as it offers, together with the presence of self-phase modulation (SPM), better handling of accumulated nonlinearity and broader spectral bandwidth, thus avoiding the fission effect [15]. To exploit the benefits, a normal dispersion Tm-doped fiber (NDTDF) based on high Ge-doping and a small core was reported. However, its amplifier performance was poor, and only 2.6 nJ was achieved at a wavelength of 1865 nm [16].

Very recently, we have reported a W-type silica TDF with normal dispersion above 1600 nm. With the W-type NDTDF, we have demonstrated an all-fiber pulsed laser and amplifier at 1850 nm up to pulse energy of 525 nJ [17]. Intriguingly, the W-type fiber exhibits a distributed short-pass filtering effect by applying bend loss, as the occurrence in W-type Erbium-doped fiber for S-band operation [18], or 3-level laser operation in Neodymium-doped fiber [19]. In this paper, by concurrently utilizing the bending-induced bandpass effect and the normal dispersion from the in-house fiber, we report a broadband tunable mode-locked TDFL in the 1740-1892 nm region from a semiconductor saturable absorber mirror (SESAM) based laser cavity. To our best knowledge, this is the broadest tunable range for mode-locked TDFL in a single cavity. To fully exploit the normal dispersion potential of the W-type NDTDF as a gain medium, we also built an all-fiber amplifier in a 1700-1800 nm region without any external filters or pulse stretcher. With optimization of the bandpass effect of the W-type NDTDFs in oscillator seed and amplification stage, pulsed laser at 1750 nm with pulse energy of 32.7 nJ and a repetition rate of 5.5 MHz was achieved without pulse breaking, which marks the first demonstration of all-fiber amplifier with TDF in the 1700 nm region, to our best knowledge. We will describe fiber details and the experimental details in the following.

2. Fiber characterization of W-type NDTDF

Our in-house fabricated W-type NDTDF has a core diameter of 5.0 μm, Tm^{3+} doping concentration of 0.35 wt. % and a core absorption of ~17.65 dB/m at 1565 nm. It is co-doped with Aluminium (Al) to disperse the dopant of Tm. The W-type NDTDF shows a cutoff wavelength of 1455 nm, which ensures a single mode operation (LP_{01} mode) in both the in-band pump wavebands and the $^3F_4$-$^3H_6$ emission region. The W-type refractive index profile (RIP) as represented in Fig. 1 enables the normal-dispersion property in the Tm emission region of 1600-2100 nm [17]. In addition, the W-type index profile also renders the distributed short-pass filtering effect, thus allowing short wavelength operation by the fiber bending technique [18]. The fabricated fiber exhibits imperfection due to fabrication tolerance such as the elliptical core as illustrated in Fig. 1(a) and Fig. 1(b). We use the measured 2-D RIP (Fig. 1(b)) to calculate the characteristics of depressed-cladding and normal-dispersion by employing a finite-element method via a commercial software, COMSOL. A 5 m long fiber is assumed and various bending

Optics EXPRESS

diameters are applied in the simulation to check bending dependence of dispersion as well as the bandpass effect.

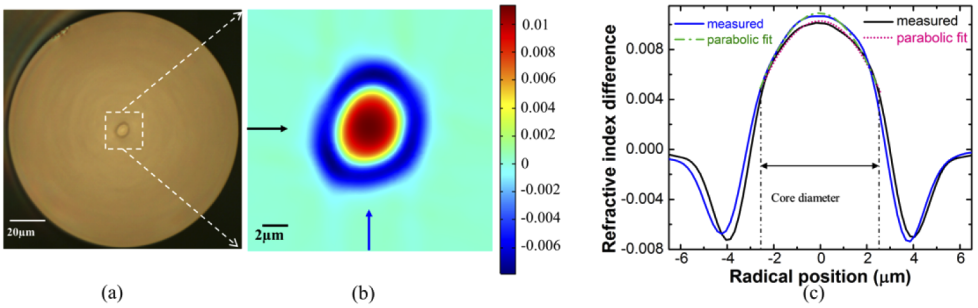

Fig. 1. (a) Cross sectional view of the fabricated W-type NDTDF under optical microscope; (b) Measured 2-D RIP of the fabricated W-type NDTDF by index profiler (IFA-100) in the section outlined by white dash line in (a); (c) Measured 1-D RIP curves of the fabricated W-type NDTDF along two perpendicular directions (labelled by arrows in (b)) and the corresponding parabolic fits in the core area.

As depicted in Fig. 2(a), the spectral bend loss is greatly influenced by the bending diameter in that tighter bending induces a blue shift of the sharp rise of bend loss. Therefore, the W-type NDTDF itself performs as a distributed short-pass filter, and the short-pass cutoff wavelength (λ_{cutoff}, as marked by solid dots) is adjustable in a broad range of 1740-1940 nm by simply changing the bending diameter. The simulation results are clearly supported by the measured backward ASE spectra from a 5 m W-type NDTDF as presented in Fig. 2(b). The ASE peak is blue-shifted from 1825 nm down to 1745 nm with tighter bending diameter from 30 cm down to 6 cm. More than >10 dB of suppression is achievable above the λ_{cutoff} whereas a loss below the λ_{cutoff} is insignificant. Furthermore, the W-type NDTDF has a near parabolic-profile in the core area as shown in Fig. 1(c). The parabolic profile greatly removes concerns related to bending distortion [20], allowing us to bend the fiber without core mode distortion. A mode field diameter (MFD) and power confinement of LP_{01} mode in the core are calculated to confirm this proposition. The fiber was assumed to bend along the two white arrows given in Fig. 2(c) and the bending induced distortion was averaged from the two bending orientations. As shown in Fig. 2(d) and Fig. 2(e), the MFD and the power confinement are well preserved from the tight bending in the wide range of 1700-2020 nm. In particular, the bending induced distortion is nearly absent in the short wavelengths below 1750 nm even under the tight bending diameter of 8 cm. Therefore, we conclude that the unique combination of W-type and parabolic profile in our fiber enables a robust bending-induced short-pass effect with no disruption to fundamental mode operation.

Subseqeuntly, dispersion of the fiber is investigated under bending which alters effective - index of the LP_{01} mode and the corresponding dispersion value. The same bending diameters and orientations are applied as in Fig. 2. The influence of bending on the dispersion is shown in Fig. 3, with comparison of measured dispersion value from ~25 cm straight W-type NDTDF by an in-house built interferometer [21]. The calculated dispersion is in good agreement to the measured dispersion value in the 1650-1800 nm region regardless of the bending diameters. In addition, as aforementioned (refer to Fig. 2(a)), the W-type NDTF permits a bending-induced short-pass cutoff wavelength, λ_{cutoff}. The wavelengths shorter than the λ_{cutoff} are operational while the longer wavelengths are suppressed. We also note that normal dispersion is offered over the entire spectral range of the study. Therefore, wavelength tunable normal dispersion pulses are anticipated from the W-type NDTDF by simply applying fiber bending.

Optics EXPRESS

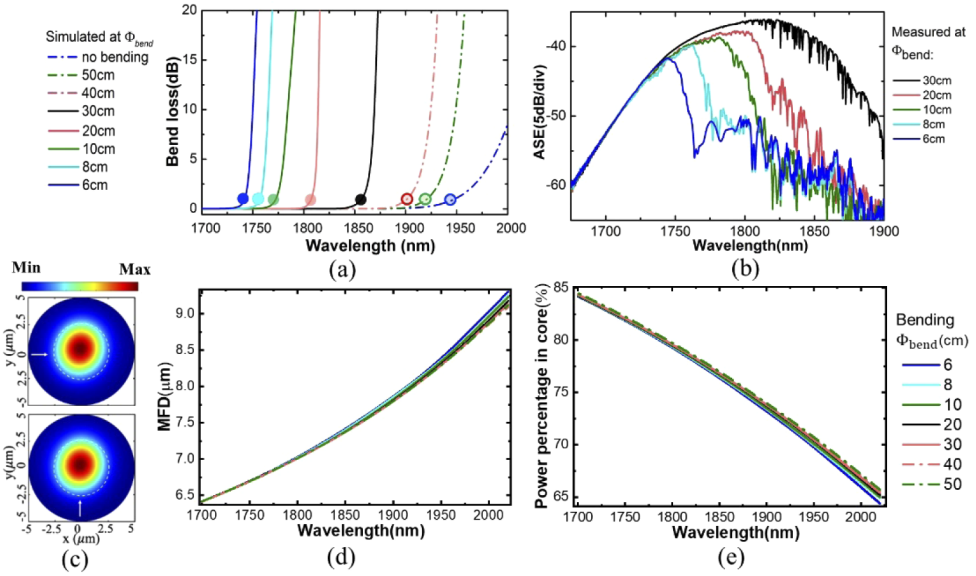

Fig. 2. (a) The averaged bend loss (along two perpendicular directions shown by arrows in Fig. 1(b)) of fabricated 5 m W-type NDTDF at different bending diameters (Φ_{bend}), calculated using COMSOL, with the respective cut-off wavelength (λ_{cutoff}) marked by solid dots; (b) measured backward ASE of the fabricated 5 m W-type NDTDF at different bending diameters (Φ_{bend}); (c) the calculated LP_{01} mode intensity profile of the W-type NDTDF at 1750 nm by bending along two perpendicular directions as indicated by white arrow (Φ_{bend} at 8 cm, white dash line represents the designed core diameter); (d) the calculated MFD and (e) power percentage of LP_{01} mode in core of fabricated W-type NDTDF with respect to wavelength at different bending diameters.

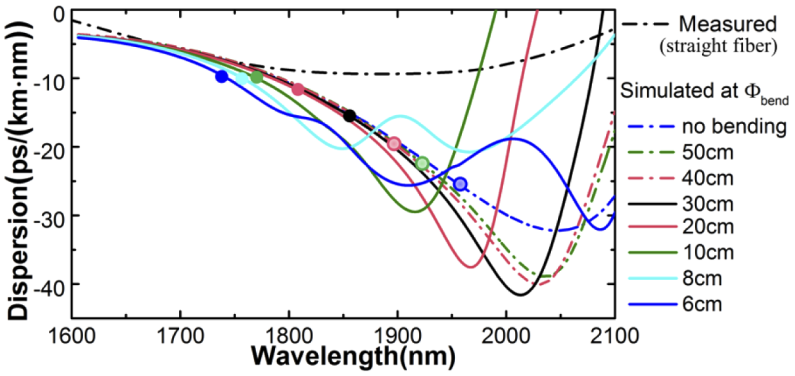

Fig. 3. Dispersion curves at different bending diameters, with the respective λ_{cutoff} marked by solid dots.

3. Experimental setup and results

The setup of all-fiber mode-locked laser oscillator and amplifier is shown in Fig. 4. The main part of the oscillator is a unidirectional ring cavity, comprising two filter-based 1550/1950 nm wavelength division multiplexers (WDMs), a polarization controller (PC), a 1900 nm polarization independent isolator (ISO), and a 1.5 m W-type NDTDF. The pump source of oscillator is composed of a tunable external cavity laser (ECL, 1480 nm -1580 nm) operating at 1565 nm

Optics EXPRESS

amplified by an Erbium-doped fiber amplifier (EDFA, Keopsys) with maximum output power of 2 W, which is launched into the cavity through WDM_1. A residual pump is out-coupled via WDM_2. The unidirectional ring cavity is coupled through a 55% port of 2×2 45/55 1950 nm coupler to a SESAM, which was placed very close to the SMF_2 end. Mode-locked signal pulses are directed to the amplifier stage via the other 45% port. To achieve higher gain at a short wavelength, we employed a backward pumping scheme in the amplification stage wherein a length of 5 m W-type NDTDF is incorporated for sufficient gain and large normal-dispersion value. A 1565 nm CW fiber laser (Keopsys) is used as the pump source of the amplifier. To stop backward residual pump and ASE from the amplification stage, a 1550 nm isolator and another 1940 nm isolator (ISO_2) are employed between the 45% port of the coupler and the 5 m W-type NDTDF. Despite the mismatched mode field area between the NDTDF and SMF-28, we were able to achieve a 0.8 dB splicing loss by optimizing splicing parameters of a conventional electric arc based fiber splicer. All the passive components are pigtailed with SMF-28. The signals before and after amplification were characterized in frequency and time domains. An optical spectrum and output power of the oscillator and amplifier were measured by an optical spectrum analyzer (OSA, Yokogawa 6375) and a power meter (Thorlabs S314C), respectively. Signal pulse trains were monitored with a digital oscilloscope (Tektronix DPO7104) along with an InGaAs photodetector (DET10D2, Thorlabs), and pulse duration was characterized by an autocorrelator (FR-103HP).

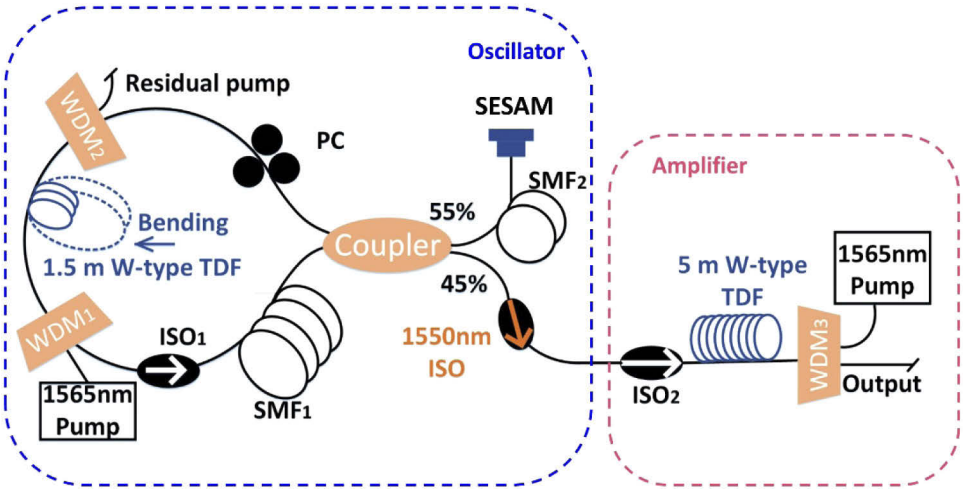

Fig. 4. Schematic of all-fiber W-type NTDF based master oscillator power fiber amplifier; the oscillator and the amplifier setups are separately outlined by dash lines. WDM: wavelength division multiplexer; ISO: isolator; PC: polarization controller; SMF: single mode fiber; SESAM: semiconductor saturable absorber mirror.

3.1. Tunable mode-locked fiber oscillator

This section presents performance of the mode-locked oscillator given in Fig. 4. The oscillator is able to generate wavelength tunable mode-locked pulses. The wavelength tunability was realized by the bending-induced filtering effect of the W-type NDTDF. It is worth noting that our tuning mechanism is different from the Lyot filtering effect in nonlinear polarization rotation (NPR) based mode-locked fiber laser [22]. As illustrated in Fig. 2, the short-pass cutoff wavelengths of our W-type NDTDF is adjustable from 1740 nm to 1950 nm by applying fiber bending. To maximize the broadband emission of a TDF in the $^3F_4$-$^3H_6$ transition, we engaged two SESAMs (SAM-1960-54-10ps and SAM-1920-36-10ps, Batop) depending on desired operating

Optics EXPRESS

wavelengths, i.e. 1740–1810 nm or 1810–1900 nm, respectively. Hence, the two SESAMs allow us to explore broadband tunability in 1740-1900 nm. We also note that the NDTDFs were placed on a heat sink, and all fibers were taped to stabilize the system.

With a larger bending diameter (Φ_{bend}) of ~50 cm of the W-type NDTDF, a stable mode-locking was achieved at 1892 nm by properly rotating PC with pump power of 29 dBm. Its repetition rate was measured of 3 MHz as a result of the cavity length of 69.5 m. By tightening the bending, lasing wavelength was shifted to short wavelength accordingly. With the pump power of 29 dBm-29.5 dBm, tunable mode-locked pulses in the 1825-1892 nm region were obtained by gradually reducing the Φ_{bend} from ~50 cm down to ~30 cm. The corresponding spectra are presented in Fig. 5(a). To further move the lasing wavelength to shorter wavelength, we engaged the short-wavelength SESAM (SAM-1960-54-10ps) in the cavity and the Φ_{bend} of W-type NDTDF was further decreased. As a result, a 1740-1803 nm tunable mode-locking was realized with the Φ_{bend} gradually reduced from 20 cm to 6 cm, with stronger pump power of 30 dBm to 30.8 dBm. The short wavelength operation requires the higher pump power due to the three-level nature of $^3F_4$-$^3H_6$ transition (increasing absorption cross section with decreasing emission cross section as shown in Fig. 5(b)). Overall, we have achieved a tunable mode-locked fiber laser with a broad tunability of 152 nm from 1740 nm to 1892 nm. The obtained pulses are soliton as indicated in Fig. 5(a). The output power at the achieved wavelength range is presented in Fig. 5(b) with required pump power to overcome the stronger absorption crosssection toward the shorter wavelength (See the blue lines).

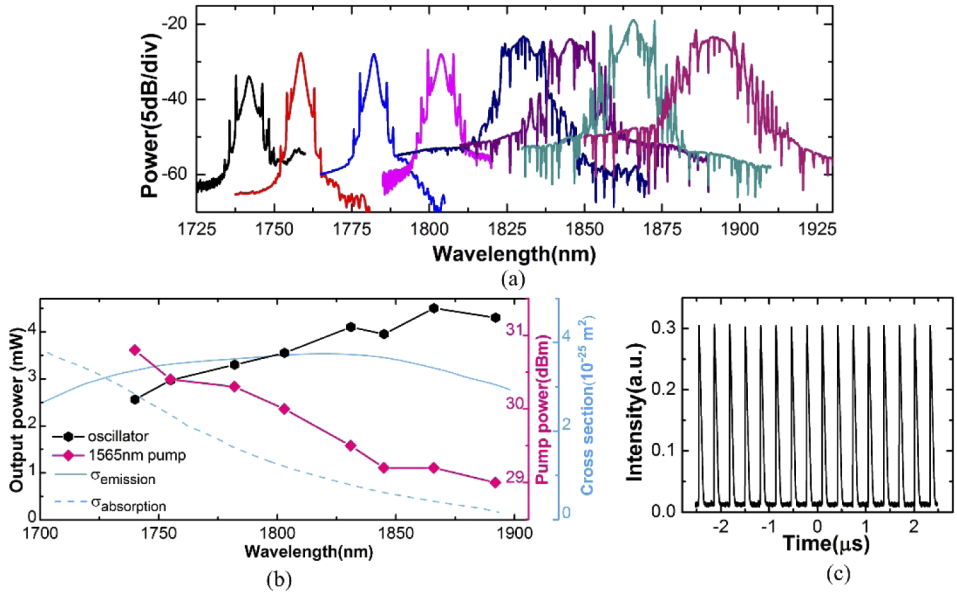

Fig. 5. (a) Tunability of the mode-locked cavity from 1740 nm to 1892 nm utilizing the W-type NDTDF ; (b) output powers at the different operating wavelengths in (a) and their corresponding pump powers (blue lines: representative absorption, $\sigma_{absorption}$, and emission, $\sigma_{emission}$, cross sections of a commercial TDF [23]); (c) a representative pulse train of the tunable mode-locked fiber lasers at 1755 nm.

3.2. *Amplification of short-wavelength mode-locked pulses*

The achieved mode-locked pulses from the oscillator was amplified through the W-type NDTDF. We built an all-fiber TDF based short-wavelength soliton amplifier without any artificial short-pass filter or pulse stretcher, with the configuration shown in Fig. 4. The bend-induced distributed

Optics EXPRESS

short-pass filtering effect of our NDTDF was utilized in the amplification to build optical gain in a desired wavelength. To reduce the impact of Kelly sidebands while being amplified in the amplifier stage, we removed a length of SMF-28 from the section of SMF_1 in the oscillator cavity. Owing to the large anomalous dispersion in SMF-28, the cavity was still in the anomalous dispersion regime. At a bending diameter of 8 cm of the W-type NDTDF, and a pump power of 30.3 dBm, a stable self-started mode-locked fiber laser at 1755 nm with an output power of 3.2 mW was obtained by properly adjusting the PC. The soliton pulse spectrum from the shortened oscillator is represented in Fig. 6(a). As intended, the sidebands are greatly reduced as compared to Fig. 5(a). In addition, the full-width half maximum (FWHM) of the spectrum in Fig. 6(a) is 2.6 nm, which corresponds to a transform-limited pulse duration of 1.74 ps for a Gaussian pulse profile (due to low peak power of the oscillator seed, we were not able to directly measure the pulse duration by an autocorrelator). Figure 6(b) shows the pulse train at the pump power of 30.5 dBm. The measured pulse-to-pulse separation is 181.8 ns, which corresponds to the cavity length of 37.8 m, indicating a repetition rate of 5.5 MHz.

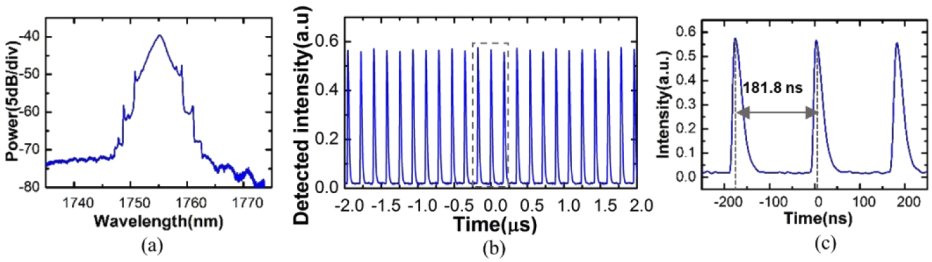

Fig. 6. (a) Optical spectrum of mode-locked soliton pulse at 1755 nm; (b) an oscilloscope trace of the pulse train at 1755 nm with pump power of 30.5 dBm and at the bending diameter of 8 cm of the W-type NDTDF and (c) the detailed pulse train with a pulse interval of 181.8 ns in the section outlined by dash line in (b).

In the amplification stage, a length of 5 m W-type NDTDF was employed at the same bending diameter of 8 cm as in the oscillator, thus having the ASE peak matched with the oscillator around 1755 nm. To construct a backward pumping scheme, a WDM_3 is introduced at the output end of the NDTF to connect the pump source. The pigtailed SMF-28 length in WDM_3 is around 0.7 m, which exhibits an anomalous dispersion of 19.2 fs/nm at 1755 nm [24]. The engaged 5 m W-type NDTDF possesses dispersion of −39.1 fs/nm at 1755 nm according to Fig. 3 (measured in a straight fiber). Considering the bending diameter of 8 cm, the corresponding total dispersion including the NDTF and the SMF-28 is expected to be < -19.9 fs/nm, hence imposing normal dispersion amplification. Figure 7(a) shows measured spectral evolution of soliton amplification as a function of the pump power. With the increase of backward pump power, it was observed that the spectral FWHM of the soliton after amplification was gradually broadened. Particularly, at the pump power of 33 dBm, SPM is clearly visible after the 5 m W-type NDTDF thanks to the local contributions of the sufficient gain, normal dispersion and high nonlinearity of the W-type NDTF. The corresponding spectral FWHM was recorded as 10.5 nm after WDM_3. It should be noted that despite the increase of pump power, the ASE in 1720-1780 nm was at least 20 dB below the amplified soliton signal. In addition, the distributed short-pass filtering effect of the bent 5 m W-type NDTDF suppressed the longer wavelength ASE more effectively. It is estimated that the output powers of amplified solitons contained more than 95% of the total output powers based on integration of the amplified spectra. Figure 7(b) shows the output power of the amplified soliton after WDM_3 as a function of launched pump power. We note that the splicing loss and the insertion loss of WDM_3 were not deducted in the plot. In other word, the actual signal power could be higher. The output power increases linearly with pump power,

Optics EXPRESS

resulting in a slope efficiency of 14.3% with respect to the launched pump power. Again, the actual efficiency could be higher when considering net efficiency after deducting the losses in the amplification stage including the 0.8 dB splicing loss per splice and the ~1 dB insertion loss of WDM_3 at the signal wavelength. The high absorption cross section at 1755 nm is another reason for the relatively low efficiency. We estimate 20 dB/m of small signal absorption at 1755 nm. As a result, high pump power was required in the amplification to overcome the reabsorption. At the pump power of 33 dBm (maximum available power), the output power of the amplifier reached ~180 mW, corresponding to a 17.5 dB gain. Moreover, thanks to the normal dispersion in the W-type NDTDF, the amplified pulses did not undergo pulse break-up, confirmed by the consistent repetition rate before and after the amplification. The measured pulse duration was slightly broadened due to the normal dispersion. Figure 7(c) shows the measured pulse duration after WDM_3 at the pump power of 33 dBm. The pulse is Gaussian with a pulse duration of 2.76 ps. Therefore, the time-bandwidth product is 2.83, showing that the pulse is chirped after propagation through the amplifier. With the measured output power of ~180 mW and the pulse duration, we have achieved a pulse energy of 32.7 nJ, corresponding to a peak power of 12.1 kW.

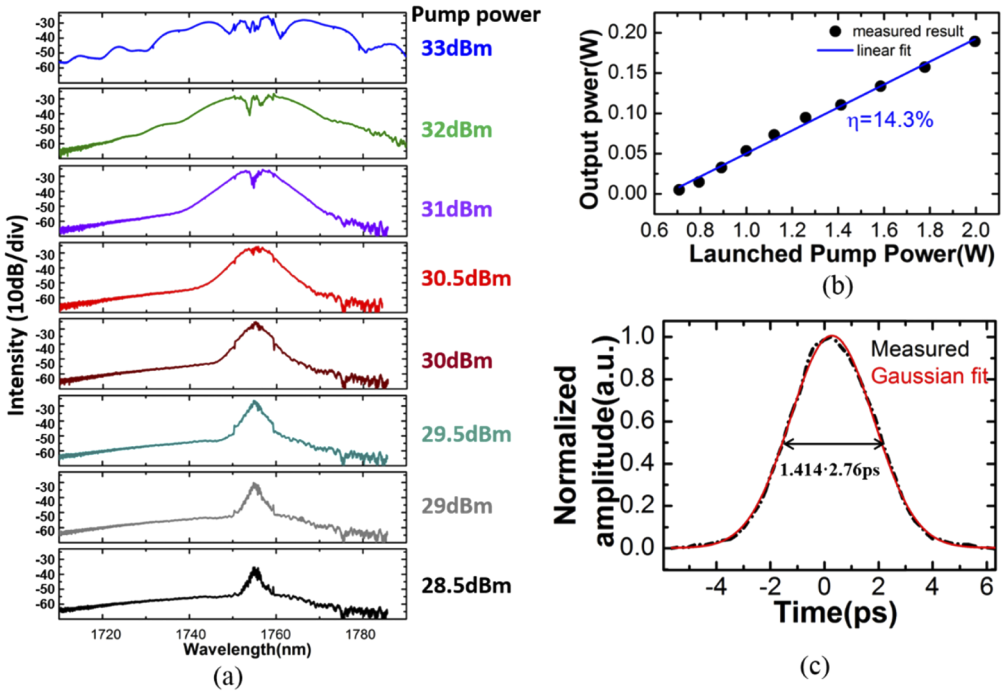

Fig. 7. (a) Spectra of amplified pulses with respect to pump power; (b) the output power (after WDM_3) versus launched pump power; (c) the measured autocorrelator trace at the full power.

In Table 1, we present a comparison of key performances of our laser and its amplification with prior works in the 1700-1800 nm region. In [14], short wavelength operation was obtained using a dichroic mirror and a bend-loss induced DCF as short-pass filters. Additionally, a length of DCF as a pulse stretcher was employed to boost pulse energy in the power amplification stage. Although the amplifier made use of a long-wavelength 1650 nm Raman laser as a pump source to improve the amplifier efficiency, the gain was eventually limited by the mismatch between the central wavelength of oscillator (1785 nm) and the longer wavelength ASE peak through a length of TDF in the amplifier. The similar issues hindered pulse energy scaling in [25]. Using a

Optics EXPRESS

normal dispersion bismuth-doped fiber (NDBDF), Khegai et al. built an all-fiber chirped pulse amplification system around 1700 nm without any help of short-pass filter or pulse stretcher [26]. However, the amplified pulse experienced high nonlinearity in the substantially long fiber length of NDBDF, which in turn degraded the pulse compression. Similarly, our work enabled all-fiber MOPA system construction that emitted 32.7 nJ pulse energy in a 2.76 ps pulse. We note that our reported result could be improved further by using customized 1750 nm passive fiber components such as WDM. In addition, a sub ps pulse duration is envisaged by introducing a compression stage which can be fiber-based.

Table 1. Main characteristics of the state-of-the-art mode-locked fiber lasers and their amplifications in the 1700-1800 nm region

Oscillator stage		Amplifier stage				Output	Ref.
Mode-locking method ($\lambda_{central}$)	Used short bandpass filter		Used pulse stretcher	Gain fiber (length)	Slope efficiency (pump wavelength)	Pulse energy, repetition rate (**configuration**)	
NPR (1785 nm)	DM	DCF	DCF	commercial TDF (2.8 m)	~27.7 % (1650 nm)	~14.9 nJ, 46.375 MHz (not all-fiber)	[14]
Raman shift soliton (1750 nm)	no filter	1750 nm spectral filter	DCF	commercial TDF (0.9 m)	~4.3 % (1550 nm)	~20 nJ, 1-6 MHz (not all-fiber)	[25]
NALM (1700 nm)	no filter		no pulse stretcher	high-Ge NDBDF (100 m)	~4.0 % (1570 nm)	~5.7 nJ, 3.57 MHz (all-fiber)	[26]
SESAM (1755 nm)	no filter		no pulse stretcher	W-type NDTDF (5 m)	~14.3 % (1565 nm)	~32.7 nJ, 5.5 MHz (all-fiber)	this work

(DM: dichroic mirror; DCF: dispersion compensating fiber; NDBDF: normal dispersion bismuth-doped fiber; NALM: nonlinear amplifying loop mirror)

4. Conclusion

An all-fiber ps oscillator and amplifier system was demonstrated for broadband tunable mode-locking and high pulse energy extraction in the short wavelength of Tm emission band, enabled by the in-house W-type NDTDF. The unique characteristics of the fiber include the immunity to bending distortion realized by a parabolic index profile, and the distributed short-pass filtering effect and normal dispersion attained by a trench cladding design. By simply bending the W-type NDTDF in a diameter of 6 cm-50 cm, a record broad tunability of mode-locked pulses was demonstrated in the range of 1740-1892 nm at a repetition rate of 3 MHz. Moreover, the W-type NDTDF exhibited a normal dispersion in the 1700-1800 nm region, allowing us to construct an all-fiber soliton fiber oscillator and amplifier around 1755 nm directly without using any external short-pass filter or additional pulse stretcher. In this all-fiber configuration, we achieved a high energy of ~32.7 nJ pulse laser around 1755 nm without pulse break-up, corresponding to a peak power of 12.1 kW in ~2.76 ps pulse.

Funding

Ministry of Education - Singapore Academic Research Fund Tier 1 (2018-T1-001-148); Sintec Optronics (S16-1257-IPP COY-15-IPP/160006).

Optics EXPRESS

Acknowledgments

Academic Research Fund Tier 1, Ministry of Education (Singapore) under Project Grant 2018-T1-001-148 (RG 84/18); EDB IPP project, Sintec Optronics Pte. Ltd. C under Grant S16-1257-IPP COY-15-IPP/160006.

Disclosures

The authors declare no conflicts of interest.

References

1. C. Xu and F. W. Wise, "Recent advances in fibre lasers for nonlinear microscopy," Nat. Photonics **7**(11), 875–882 (2013).
2. N. G. Horton, K. Wang, D. Kobat, C. G. Clark, F. W. Wise, C. B. Schaffer, and C. Xu, "In vivo three-photon microscopy of subcortical structures within an intact mouse brain," Nat. Photonics **7**(3), 205–209 (2013).
3. S. P. Chong, C. W. Merkle, D. F. Cooke, T. Zhang, H. Radhakrishnan, L. Krubitzer, and V. J. Srinivasan, "Noninvasive, in vivo imaging of subcortical mouse brain regions with 1.7 μm optical coherence tomography," Opt. Lett. **40**(21), 4911–4914 (2015).
4. M. Yamanaka, T. Teranishi, H. Kawagoe, and N. Nishizawa, "Optical coherence microscopy in 1700 nm spectral band for high-resolution label-free deep-tissue imaging," Sci. Rep. **6**(1), 31715 (2016).
5. C. Li, J. Shi, X. Gong, C. Kong, Z. Luo, L. Song, and K. K. Y. Wong, "1.7 μm wavelength tunable gain-switched fiber laser and its application to spectroscopic photoacoustic imaging," Opt. Lett. **43**(23), 5849–5852 (2018).
6. J. M. O. Daniel, N. Simakov, M. Tokurakawa, M. Ibsen, and W. A. Clarkson, "Ultra-short wavelength operation of a thulium fibre laser in the 1660–1750 nm wavelength band," Opt. Express **23**(14), 18269–18276 (2015).
7. K. Wang and C. Xu, "Tunable high-energy soliton pulse generation from a large-mode-area fiber and its application to third harmonic generation microscopy," Appl. Phys. Lett. **99**(7), 071112 (2011).
8. T. Noronen, S. Firstov, E. Dianov, and O. G. Okhotnikov, "1700 nm dispersion managed mode-Locked bismuth fiber laser," Sci. Rep. **6**(1), 24876 (2016).
9. S. Firstov, S. Alyshev, M. Melkumov, K. Riumkin, A. Shubin, and E. Dianov, "Bismuth-doped optical fibers and fiber lasers for a spectral region of 1600–1800 nm," Opt. Lett. **39**(24), 6927–6930 (2014).
10. T. Noronen, O. Okhotnikov, and R. Gumenyuk, "Electronically tunable thulium-holmium mode-locked fiber laser for the 1700-1800 nm wavelength band," Opt. Express **24**(13), 14703 (2016).
11. S. Chen, Y. Jung, S. Alam, D. J. Richardson, R. Sidharthan, D. Ho, S. Yoo, and J. M. O. Daniel, "Ultra-short wavelength operation of thulium doped fiber amplifiers and lasers," Opt. Express **27**(25), 36699–36707 (2019).
12. S. D. Emami, M. M. Dashtabi, H. J. Lee, A. S. Arabanian, and H. A. A. Rashid, "1700 nm and 1800 nm band tunable thulium doped mode-locked fiber lasers," Sci. Rep. **7**(1), 12747 (2017).
13. C. Huang, C. Wang, W. Shang, N. Yang, Y. Tang, and J. Xu, "Developing high energy dissipative soliton fiber lasers at 2 micron," Sci. Rep. **5**(1), 13680 (2015).
14. C. Li, X. Wei, C. Kong, S. Tan, N. Chen, J. Kang, and K. K. Y. Wong, "Fiber chirped pulse amplification of a short wavelength mode-locked thulium-doped fiber laser," APL Photonics **2**(12), 121302 (2017).
15. M. Tokurakawa, H. Sagara, and H. Tünnermann, "All-normal-dispersion nonlinear polarization rotation mode-locked Tm:ZBLAN fiber laser," Opt. Express **27**(14), 19530–19535 (2019).
16. D. Klimentov, V. V. Dvoyrin, and I. T. Sorokina, "Mode-Locked Thulium-Doped Fiber Lasers Based on Normal Dispersion Active Fiber," IEEE Photonics Technol. Lett. **27**(15), 1609–1612 (2015).
17. Y. Chen, S. Chen, R. Sidharthan, C. J. Cheng, K. Liu, S. Rao. D. S., O. Bang, Q. J. Wang, D. Tang, and S. Yoo, "High Energy Ultrafast Laser at 2 μm Using Dispersion engineered Thulium-Doped Fiber," IEEE Photonics J. **11**(6), 1–12 (2019).
18. M. Foroni, F. Poli, A. Cucinotta, and S. Selleri, "S-band depressed-cladding erbium-doped fiber amplifier with double-pass configuration," Opt. Lett. **31**(22), 3228–3230 (2006).
19. S. Yoo, D. B. S. Soh, J. Kim, Y. Jung, J. Nilsson, J. K. Sahu, J. W. Lee, and K. Oh, "Analysis of W-type waveguide for Nd-doped fiber laser operating near 940 nm," Opt. Commun. **247**(1-3), 153–162 (2005).
20. J. Sun, Z. Kang, J. Wang, C. Liu, and S. Jian, "Novel bending-resistant design of two-layer low-index trench fiber with parabolic-profile core," Opt. Express **22**(15), 18036–18043 (2014).
21. W. Qi, X. Huang, D. Ho, S. Yoo, K. T. Yong, and F. Luan, "Dispersion measurement of optical fibers by phase retrieval from spectral interferometry," J. Opt. **19**(5), 055611 (2017).
22. B. Sun, J. Luo, Z. Yan, K. Liu, J. Ji, Y. Zhang, Q. J. Wang, and X. Yu, "1867–2010 nm tunable femtosecond thulium-doped all-fiber laser," Opt. Express **25**(8), 8997–9002 (2017).
23. S. D. Agger and J. H. Povlsen, "Emission and absorption cross section of thulium doped silica fibers," Opt. Express **14**(1), 50–57 (2006).
24. P. Ciąćka, A. Rampur, A. Heidt, T. Feurer, and M. Klimczak, "Dispersion measurement of ultra-high numerical aperture fibers covering thulium, holmium, and erbium emission wavelengths," J. Opt. Soc. Am. B **35**(6), 1301 (2018).

Optics EXPRESS

25. A. Wienke, D. Wandt, J. B. Lecourt, D. Lekime, Y. Hernandez, J. Neumann, and D. Kracht, "High energy, femtosecond fiber laser source at 1750 nm for 3-photon microscopy (Conference Presentation)," Proc. SPIE **10683**, 106831T (2018).
26. A. Khegai, M. Melkumov, K. Riumkin, V. Khopin, S. Firstov, and E. Dianov, "NALM-based bismuth-doped fiberlaser at 1.7μm," Opt. Lett. **43**(5), 1127–1130 (2018).

202.196.80.46 (to 2020-06-08 04:29:02)